DEUTSCHES ELEKTRONEN-SYNCHROTRON DESY

DESY 86-079
July 1986

CHROMATIC CORRECTIONS AND DYNAMIC APERTURE IN THE HERA ELECTRON RING I

by

R. Brinkmann and F. Willeke

Deutsches Elektronen-Synchrotron DESY, Hamburg

ISSN 0418-9833

NOTKESTRASSE 85 · 2 HAMBURG 52

To be sure that your preprints are promptly included in the
HIGH ENERGY PHYSICS INDEX ,
send them to the following address (if possible by air mail) :

DESY
Bibliothek
Notkestrasse 85
2 Hamburg 52
Germany

DESY 86-079
June 1986

ISSN 0418-9833

Chromatic Corrections and Dynamic Aperture in the HERA Electron Ring

I

R. Brinkmann and F. Willeke
Deutsches Elektronen-Synchrotron DESY

Abstract

Achromatic optical solutions for the HERA e^--ring are presented and discussed. The dynamic aperture for the three different optics is studied by particle tracking and perturbation theory.

We found a significant advantage of quasi-superperiodic solutions with respect to the non-periodic solutions and an advantage of a 6-sextupole family solution with respect to a 2-family solution.

The sextupole acceptance for the preferred optical solution is as large as 27 standard deviations at a beam energy of 35 GeV.

1. Introduction

In the HERA electron ring - like in most electron machines - sextupole fields needed to compensate chromatic effects are an important contribution to the non-linear forces, which determine the dynamic aperture. The strength of the sextupole fields necessary to compensate the chromaticity depends on the size of the dispersion function which, on the other hand, determines the emittance generation by photon emission in the arcs. The chromaticity scales with the inverse beam size at the interaction point which determines, together with the beam emittance, the maximum achievable luminosity for a given beam intensity. Thus, high luminosity is in conflict with large dynamic aperture not only due to the non-linear forces of the beam-beam interaction but also because of the necessary high sextupole fields.

In this report we investigate the dynamic aperture limit in the HERA electron ring using optics for luminosity operation with a phase advance of 60° per cell in the FODO-lattice arcs. These optics are based on the actual HERA lattice[1] which has no superperiodicity: Three quadrants have straight sections designed for electron-proton head-on collision whereas the fourth straight section (in the west quadrant) is reserved for utilities (injection, proton dump, etc.).

The chromatic effects in these optics have been corrected with up to 6 sextupole families as it has been proposed in reference[2].

In particular, we are interested in the following questions:

*) How does the dynamic aperture of a sextupole configuration with 6 families compare with the dynamic aperture of a 2-family distribution?

*) How important are quasi-superperiodic optical solutions, where at least in linear approximation the ideal machine appears to have superperiodicity?

*) Is it possible to understand the results obtained by simulation in terms of the theory of non-linear dynamics?

The investigation is done in four steps:

First, a linear optics solution is generated based on the optical design described in reference 1).

Then up to 2 x 6-sextupole families are introduced in the design in an interleaved correction scheme and the strengths of the sextupoles are adjusted to compensate the linear chromaticity and to eliminate the change of the envelope functions at the interaction points. These procedures and results are described in section 2.

We use the tracking code RACETRACK[3] to find the dynamic aperture as a function of tunes and energy amplitudes for these optical solutions. The tracking procedure and modifications of the standard tracking code are described in section 3.

Tracking results will be compared with analytical calculations of driving terms, detuning terms and phase space distortions. Discussion of the results is presented in section 4.

There are three optical solutions which are compared:

The preferred solution has a quasi-threefold superperiodicity. This is achieved by an integer betatron phase advance in both planes through the whole west quadrant. Thus, the transfer matrix between the symmetry points in the center of the north-west arc and south-west arc is a unity matrix. For each quadrant, 6-sextupole families are used to compensate the linear chromatic effects (denoted by SHA, SHB, SHC and SVA, SVB, SVC).

This optical solution is compared with a design with non-integer phase advances through the west quadrant, but with the same sextupole correction scheme.

The third optics solution also has the quasi-threefold symmetry but only 2-sextupole families are used to compensate the linear chromaticity.

2. Linear Optics and Sextupole Distribution

Basically, the optics investigated here are those described in reference 1)*). The optics for the three interaction sections and the special straight section west are shown in figs. 2.1 and 2.2.

Due to the asymmetry of the machine the question arises how to distribute the phase advance around the ring. We have investigated two possibilities:

a) integer phase advance in both planes for the quadrant**) west, $\Delta\Phi^{W}_{x,z} = N_{x,z}$ and $\Delta\Phi_{x,z} = (Q_{x,z} - N_{x,z})/3$ for the north, east and south quadrants.

b) equal phase advance $\Delta\Phi_{x,z} = Q_{x,z}/4$ in all four quadrants.

The optics (a) restores a "quasi-threefold" supersymmetry of the ring, which may help to suppress structure resonances not only excited by the lattice but also by the beam-beam interaction. The condition $\Delta\Phi^{W}_{x,z}$ = integer in the west quadrant can be easily met by tuning the 2-quadrupole families in the long rf-section west.

The sextupoles are distributed in the arcs according to the interleaved scheme proposed by A. Wrulich[2]. In this scheme, 24 cells per octant are used for chromaticity compensation, as sketched below:

center arc - SHC - SVC - SHB - SVB - SHA - SVA - SHC - ... - SVA -

- 1 cell - half straight section - I.P. (or center West)

The mirror symmetry of the lattice with respect to the center of the straight sections is only very slightly distorted by the fact that all sextupoles are placed downstream from the quadrupoles. We have neglected this asymmetry and we have given the sextupoles equal strengths on either side of the straight sections.

---

*) However, after introducing some readjustments of the lattice (e.g. the length of the rf-straights was changed from 5.9 to 5.6 m) we made no attempt to retain spin transparency. Spin transparency means that in linear approximation the precision of the electron spin does not depend on the transverse or longitudinal motion. But since the spin match procedure almost does not change the chromaticity of the ring, we do not expect it to have a significant influence on the chromatic and non-linear properties of the optics.

**) A quadrant is defined as the section between the symmetry points (centers) of two arcs adjacent to one straight section.

With 6-sextupole families, the transfer matrices in both planes can be made linearly independent of the momentum deviation $\Delta p/p$. Formally, this requires that the integrals determining the chromaticity and the off-energy ß-beat generated in that section vanish (i = x,z):

$$_i := \frac{1}{4\pi}\int_{s_0}^{s} dt\ \beta_i(t)[k_i(t) - m(t)\ D(t)] = 0$$

$$B_i := -\int_{s_0}^{s} dt\ \sin 2(\Phi_i(s) - \Phi_i(t))\ \beta_i(t)\cdot[k_i(t) - m_i(t)D(t)] = 0$$

$$\frac{dB_i(s)}{ds} = -2\int_{s_0}^{s} dt\ \cos 2(\Phi_i(s) - \Phi_i(t))(\beta_i(t)/\beta_i(s)[k_i(t) - m_i(t)D(t)] = 0$$

where k(s) and m(s) are the quadrupole and sextupole strengths, respectively, $\Phi(s)$ is the phase advance and ß(s) and D(s) are the amplitude and dispersion functions. The integrals in eq. (1) can easily be evaluated with an optics code. This feature has been installed in the COMFORT-code which is now able to adjust the strengths of up to 20 sextupole families to match the desired values of , B and B' (in this case, zero at interaction points and arc centers) at up to three fit points. The results of this optimization procedure are shown in Figs. 2.5 and 2.6 for the threefold symmetric optics (a) and in figs. 2.8 and 2.9 for optics (b). The chromatic behaviour of the optics with only 2-sextupole families is shown for comparison in figs. 2.3 and 2.4. In table 1 the corresponding sextupole strengths are listed. The compensation scheme with 2 x 6-sextupole families turns out to work very well for both optics. The ß-variation at the interaction points is reduced to about ± 5 % over a momentum interval of 1±%. Due to the quasi-symmetry of optics (a) the chromatic behaviour is more similar at all interaction points as for the optics (b). It should also be noted that the differences in sextupole strengths needed to compensate the off-energy ß-beat are significantly smaller for the "threefold-symmetric" optics.

Family	Optics (b) b_3 /m^{-2}	Optics (a) b_3 /m^{-2}	Note
SH	- 0.0967	- 0.0960	2-family
SV	0.1591	0.1571	distribution
SHA	- 0.1007	- 0.0703	
SHB	- 0.1389	- 0.1169	6-family
SHC	- 0.0631	- 0.1179	distribution
SVA	0.1168	0.1674	in I.P.-
SVB	0.2344	0.1806	quadrant
SVC	0.1565	0.1551	
SHAW	- 0.0771	- 0.0730	
SHBW	- 0.0697	- 0.0803	6-family
SHCW	- 0.1325	- 0.0962	distribution
SVAW	0.1655	0.1277	in West-
SVBW	0.0939	0.1092	quadrant
SVCW	0.1888	0.1511	

Table 1: Integrated sextupole strengths $b_3 = m \cdot \ell = \int ds e\beta''/p$ for optics (a) and (b) with two and six family distributions.

Figure Captions

Fig. 2.1 Linear optics of the HERA-e interaction section with spin rotator.

Fig. 2.2 Linear optics of the straight section West of the HERA electron ring.

Fig. 2.3 Energy dependence of tunes, β-, α- and dispersion functions at interaction point South (almost equivalent to interaction point North) for optics (a) with 2 sextupole families.
Solid curves : x-plane
dashed curves: z-plane

Fig. 2.4 Same as fig. 2.3, interaction point East.

Fig. 2.5 Same as fig. 2.3, optics (a) with 2 x 6 sextupole families.

Fig. 2.6 Same as fig. 2.5, interaction point East.

Fig. 2.7 Energy dependence of tunes, β-, α- and dispersion functions at interaction point South for optics (b) with 2 x 6 sextupole families.

Fig. 2.8 Same as fig. 2.7, interaction point East.

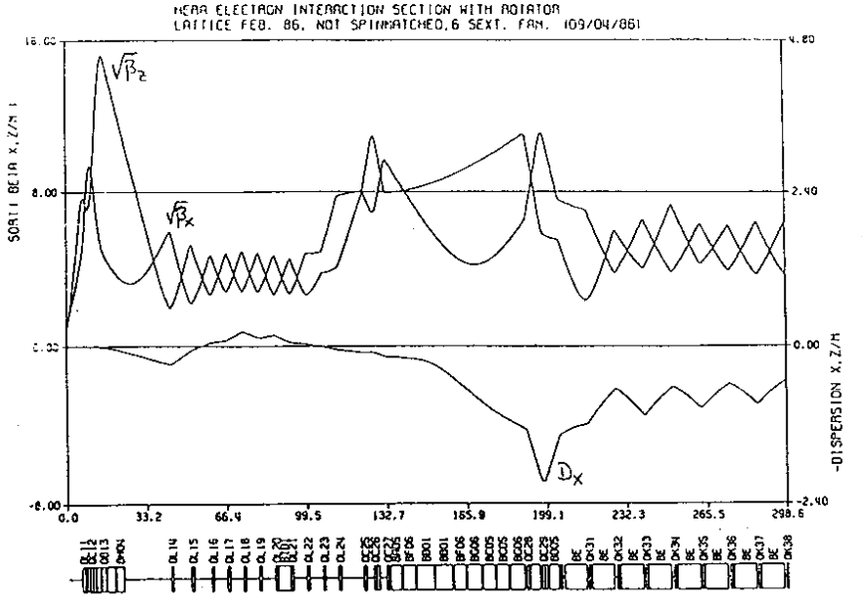

Fig. 2.1

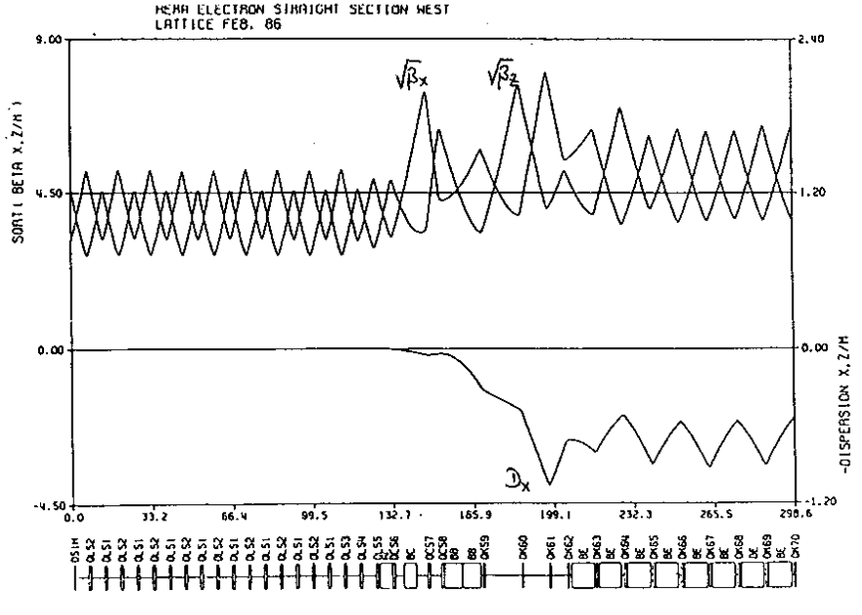

Fig. 2.2

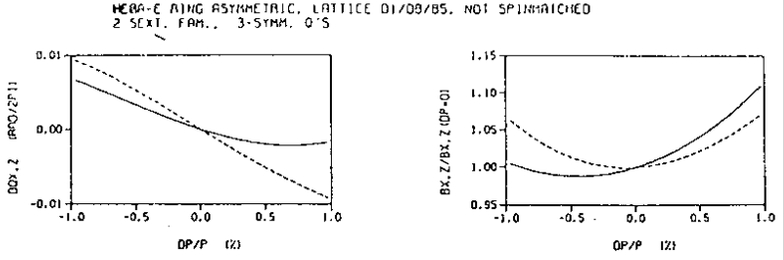

ENERGY DEPENDENCE OF OPTICS AT POINT S = IP2
TUNES: QX= 47.161 QZ= 47.279

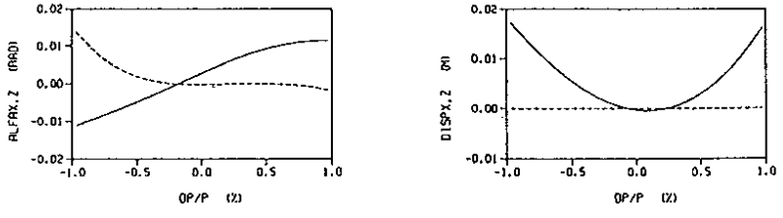

Fig. 2.3

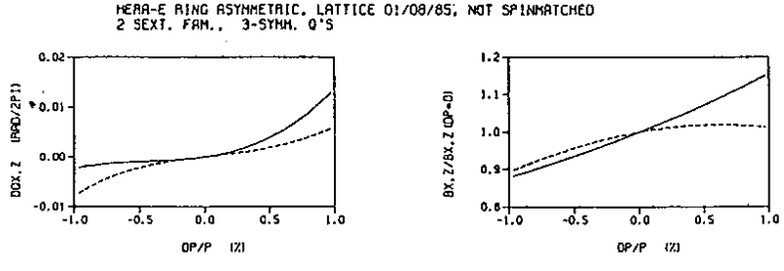

ENERGY DEPENDENCE OF OPTICS AT POINT S = END
TUNES: QX= 47.161 QZ= 47.279

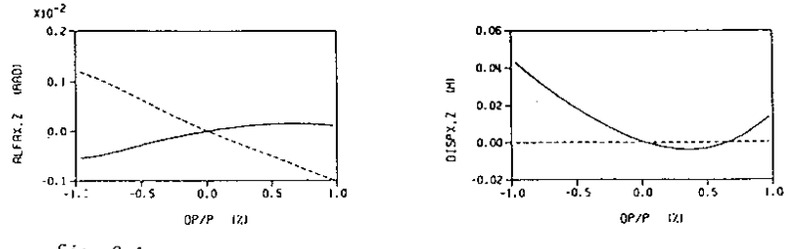

Fig. 2.4

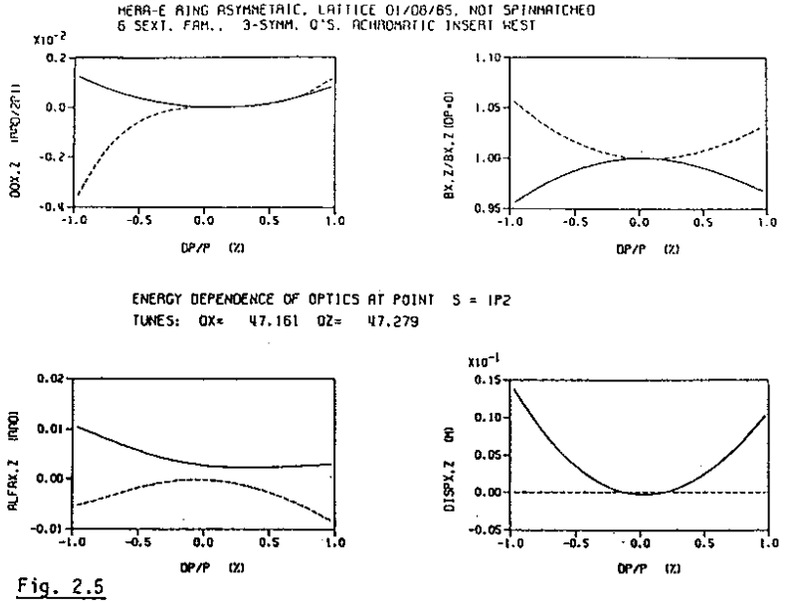

Fig. 2.5

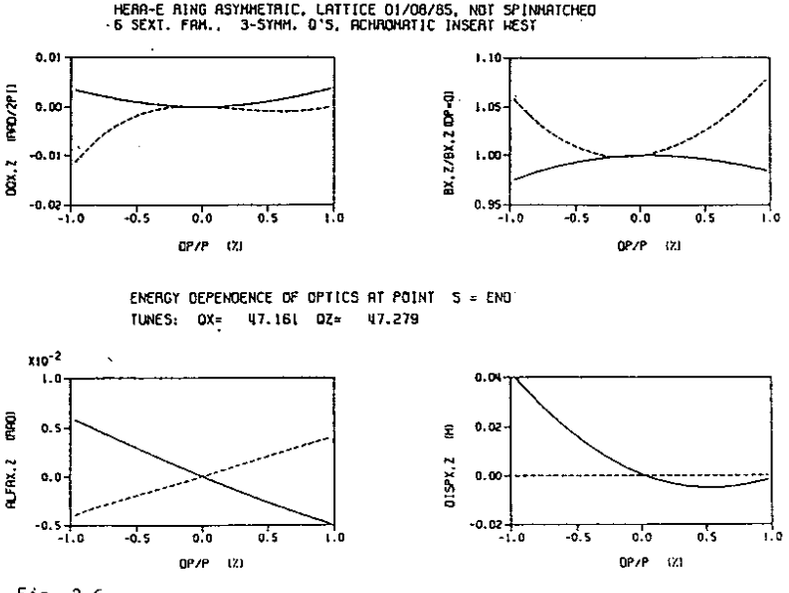

Fig. 2.6

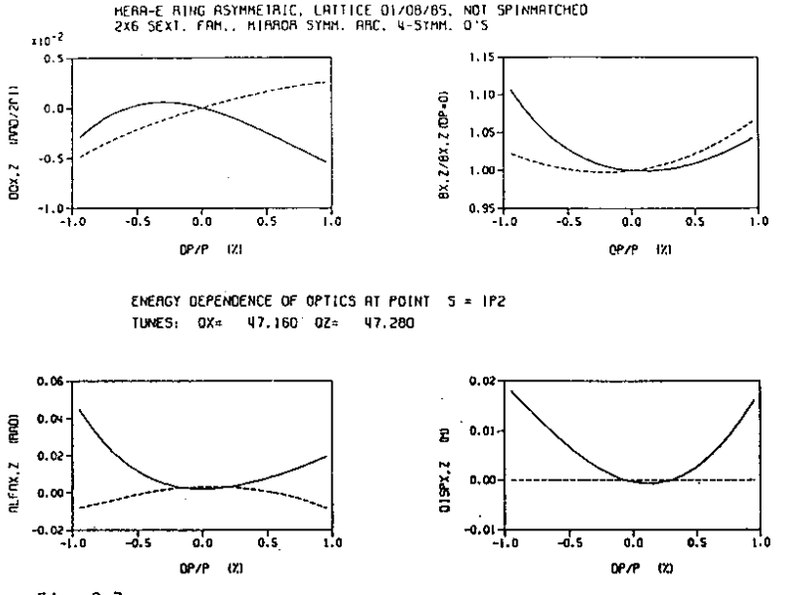

Fig. 2.7

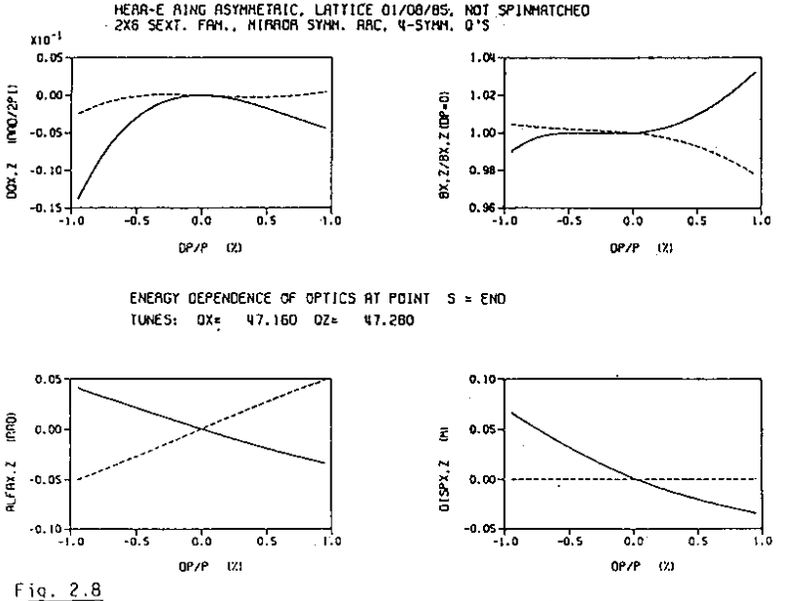

Fig. 2.8

3. Particle Tracking

The dynamic aperture for the optical solutions described in the previous section is investigated by using the tracking code RACETRACK [3]. This computer program simulates the particle motion through the storage ring by transforming the particle coordinates successively through the non-linear elements, in our case sextupole magnets. The non-linear forces are taken into account as a kick added to the trajectory slope in the middle of each sextupole magnet.

The dynamic aperture in RACETRACK is defined as the maximum start amplitude, a vector in the four dimensional phase space, which remains within a given aperture for a given number of turns around the machine. Because the length of the so-defined maximum start vector depends on its orientation in phase space, RACETRACK distributes several particles (up to 64) under different phase angles and selects the smallest maximum stable start vector for the dynamic aperture.

This definition of the dynamic aperture corresponds to the maximum stable emittance of a beam injected at the starting point of the tracking where the injection channel is perfectly matched to the linear storage ring.

For electrons at high energy, however, it gives generally too pessimistic results. That is because maximum linear hypersphere which fits in the distorted phase space is in general smaller than the available stable phase space volume, which is the acceptance. In an electron machine the acceptance is completely filled with particles due to the emittance generation by photon emissions in the arcs.

This effect may have not much practical importance for a "round" beam for which the phase space distortions, thus the deviations from a 4-dim sphere (or more generally from a 4-dim ellipsoid) are small.

For a flat beam, however, the distortions in the vertical subspace are usually very large so that the maximum vertical dynamic aperture for fixed horizontal amplitude is always underestimated.

Therefore, the RACETRACK program has been modified such that it provides now more information about the distorted phase space. The size of the stable region of the phase space is characterized by two values of generalized emittances J_x and J_z which are obtained by integrating the Courant-Snyder emittance in one oscillation plane over the phase angle in the same plane. Only coordinates with fixed phase angle in the other oscillation plane are taken into account.

This procedure is motivated by perturbation theory. The Courant-Snyder emittances ε_x, ε_z

$$\varepsilon_x = \gamma_x x^2 + 2\alpha_x x x' + \beta_x x'^2$$

are in the case with non-linear forces no invariants but vary with the Courant-Snyder phase angles Φ_x, Φ_z

$$\Phi_x = \arctan\left(\frac{\alpha_x x + \beta_x x'}{x}\right).$$

Using perturbation theory ε_x and ε_z can be expressed [4] as a function of two invariants J_x and J_z and the Courant-Snyder phase angles Φ_x, Φ_z. Thus

$$\varepsilon_{x,z} = f_{x,z}\,(J_x, J_z, \Phi_x, \Phi_z, s)$$

At a fixed position s, ε_x is a function of only Φ_x if Φ_z is kept constant.

The functions $f_{x,z}$ are perturbation series of powers of the strength of the non-linear forces.

Furthermore, the invariants $J_{x,z}$ and $\varepsilon_{x,z}$, the perturbed emittances, are related by

$$J_{x,z} = \frac{1}{2\pi} \oint d\,\Phi_{x,z}\ \varepsilon_{x,z}\,(\Phi_{x,z}, \Phi_{z,x} = \text{const})$$

The area enclosed by a phase space trajectory is therefore the natural generalization of the emittances in the linear case.

For specific ranges of the invariants J_x, J_z the functions $f_{x,z}$ don't exist as perturbation series, that is near a non-linear resonance

$$n\,Q_x\,(J_x, J_z) + m\,Q_z\,(J_x, J_z) + p \approx 0$$

$Q_x\,(J_x, J_z)$ are the amplitude dependent tunes and n, m and p are integers. In most cases, this concerns small shells of the phase space which may contain highly periodic orbits surrounded by chaotic regions.

For these regions, the procedure of determining the effective invariants is expected to give some value in between the values from the neighbouring regular trajectories.

The other advantage of this procedure is that tracking of only one particle is enough to detect a complete surface of the phase space. Thus, the information obtained by the tracking the particles turn by turn is used very effectively. Therefore, using the same amount of computing time, the particles can be traced a significantly larger number of turns, which makes the results more reliable.

The code RACETRACK can take into account synchrotron oscillations. However, the synchrotron oscillations are performed by assuming that the particle is moving along the closed orbit, thus there is no influence of the actual betatron amplitude on the synchrotron motion and therefore no feedback on the synchrotron motion*). Such a feedback is, however, a characteristic of a coupling resonance so that one can say that the effect of synchro-betatron resonances can be simulated only approximately. Since the feedback on the longitudinal motion is small this is expected to be a good approximation.

On the other hand - off resonance - there remains the important influence of tune modulation on the beam dynamics which is well simulated by the program. For the tracking with synchrotron motion the transverse invariants are formed using coordinates with respect to the closed orbit corresponding to the actual momentum deviation $\Delta p/p$.

Presentation of the results is not without difficulties. Even after we reduced the four dimensional phase space to a two-dimensional subspace by averaging the emittances over the two phase angles resulting in the invariant areas we are still left with the fact that the size of the maximum horizontal stable phase area depends very much on the size of the vertical phase area. This is illustrated in fig. 3.2 which shows the vertical maximum stable emittance versus the horizontal emittance for a HERA e^--like FODO structure. In order to reduce the two-dimensional problem to a one-dimensional one, we assume that the electron beam will always have the same ratio of horizontal and vertical emittance of 10 % (which may be an upper value for operable conditions in HERA). We assume that this ratio is independent of the amount of phase space distortion which increases with increasing phase space volume.

---

*) Recently there is also a RACETRACK version made available which includes longitudinal motion without that restriction[5].

We are well aware that is a certain approximation which is necessary to restrict the amount of computer time. Proceeding that way, there is another problem: Unfortunately, it is not possible to inject the particles such that for all runs the same ratio A_z/A_x is obtained, since the structure of the phase space near the dynamic aperture is not known at the start of the tracking. This problem could only be solved by iterating the starting point. This also would require a large expense in computing time.

So we track with a constant ratio of 10 % of the Courant-Snyder emittances for the starting points which results generally in different ratios of the invariant areas for each run. Therefore, presenting the results we always plot the value of the horizontal acceptance A_x and on top of it the corresponding vertical acceptance A_z, thus $A_x + A_z$. This is useful because often the blow-up of the vertical emittance is an effect of a coupling resonance for which $\varepsilon_x + \varepsilon_z$ is the appropriate invariant.

Even if the results obtained that way sometimes may not be so easy to interpret, they nevertheless demonstrate the advantage of the present procedure of finding the dynamic aperture compared with the standard RACETRACK procedure. The latter one would give more or less the same result for the horizontal emittance but would give the same ratio A_z/A_x for all cases, which is obviously wrong.

The tracking parameter used for all runs presented in the following sections are as follows:

Number of turns: 1000

Number of particles: 1

Number of amplitude iterations: 8

Range of momentum amplitudes: 0.8 ‰

initial ratio of emittances

(for $\Phi_x = \Phi_z = 0$) $\dfrac{\varepsilon_z(\Phi_x=\Phi_z=0)}{\varepsilon_x(\Phi_x=\Phi_z=0)}$: 10 %

Harmonic number: 10600

Synchronous phase: 45°

Momentum compaction factor: $6.4 \cdot 10^{-4}$

Accelerating voltage: 200 MV

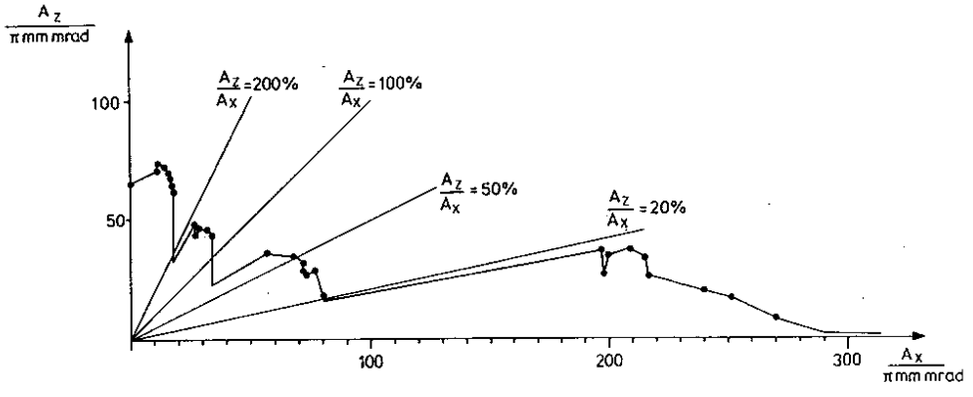

Fig. 3.1

Fig. 3.1 Non-linear acceptance for a HERA-e like FODO structure as a function of the emittance ratio A_z/A_x.

4. Results of Tracking Calculation

First, we present the tracking results for transverse motion for a fixed momentum $\Delta p/p$ in order to study the transverse effects.

In order to find an optimum working point we first performed a scan of the tunes. This also shows the different sensitivity of the different optical solutions to non-linear resonances. In figs. 4.1 to 4.3 the acceptance is plotted for different horizontal tunes in the range between Q_x = 47.08 and 47.34, for constant vertical tune Q_z = 47.28.

Plotted is the maximum horizontal acceptance A_x and the sum of maximum horizontal and vertical acceptance $A_x + A_z$ according to the ideas outlined in the previous section.

Fig. 4.1 is the result for the quasi-threefold symmetric solution with 2 sextupole families, fig. 4.2 the result for the same optics (a) with 6-sextupole families and fig. 4.3 is the result for the nonsymmetric solution (b). The 4th integer resonance $4Q_x$ = 189 imposes an important acceptance restriction for all 3 solutions. However, it is somewhat more pronounced in the cases with 6-sextupole families.

We expected such a result because of the stronger peak values of the sextupole families in these cases and the fact that the 4th integer resonance is driven by a term quadratic in the sextupole strengths.

Note that the 4th integer resonance is for both quasi-symmetric and non-symmetric cases a structure resonance, because the phase advance in the West quadrant is 12.00, thus the tune of a quasi-superperiod at a machine tune of Q_x = 47.25 is ν_x = (47.25 - 12)/3 = 11.75.

The most striking difference between optics (a) and (b) is the absence of the 3rd order resonance for the quasi-threefold symmetric solution. This shows that the unit transfer matrix of the West quadrant is retained in first order of the non-linear perturbations so that this resonance is suppressed by the superperiodicity. Our interpretation is confirmed by the phase space plots shown in figs. 4.4 and 4.5. We clearly recognize that the 4th integer resonance causes instability whereas the third integer resonance is completely stabilized by detuning.

As a consequence, the acceptance of the non-symmetric solution is reduced over the whole tune range by a factor of at least 0.6, from which one may deduce a strong preference for the supersymmetric solution. For both optics, several additional resonances could be identified (see figs. 4.1 to 4.3), which are driven by terms up to 3rd order in the sextupole strengths. This displays the disadvantage of the missing strict superperiodicity so that every higher order resonance is a structure resonance.

The value of the vertical tune used for the above runs is already very well optimized, which is confirmed by fig. 4.6 which shows the vertical Q-scan for the supersymmetric solution with 6-sextupole families.

From those results follows an optimum working point of $Q_x \approx 47.16$ and $Q_z \approx 47.28$ which is chosen for all further investigations.

The second step in the investigation of the dynamic aperture is how the variation of a fixed momentum deviation $\Delta p/p$ influences the acceptance. There are two effects, which influence the acceptance as a function of fixed $\Delta p/p$:

First, ß-functions and phase advances are distorted. These distortions generally tend to increase the driving terms of non-linear resonances because ß-functions enter with a power of at least 1.5 in the driving terms (thus, there is no cancellation of an oscillating ß-beat) and because the suppression of driving terms depends on the proper phases between non-linear elements.

In addition, a ß-beat gives rise to 2nd order chromaticity which may shift the working point towards dangerous resonances. We therefore expect better results for the 6-family solutions for which these higher order chromatic effects are better compensated.

In figs. 4.7 to 4.9 the tracking results for the three solutions (symmetric 6 families, symmetric 2 families, and non-symmetric 6 families) are shown in the range of $-1\ \% \leq \Delta p/p \leq +1\ \%$. The expectations are completely satisfied as one may conclude from the comparison of fig. 4.7 and 4.8. While for the 2-family solution the acceptance has a slope as a function of $\Delta p/p$, the 6-family solution acceptance is more flat. It is gratifying that for small momentum deviations the 6-family solution doesn't show any acceptance reduction with respect to the 2-family solution as one might suspect because of the higher sextupole peak values in the 6-family solution.

Again we find that the acceptance for the non-symmetric solution is worse over the whole momentum range. The sudden drop of the acceptance for $\Delta p/p \geq 0.4\ \%$ is hard to understand since we didn't observe strong resonances in this range of off-energy tunes. A possible explanation may be that the chromatic distortion of the optics leads to a stronger excitation of the $4Q_z = 189$ resonance towards which the vertical tune is shifted by non-linear chromaticity.

In the third step of the tracking calculations, synchrotron oscillations are taken into account. As mentioned in the previous chapter, genuine synchro-betatron resonances can't be investigated with the standard RACETRACK code because the synchrotron motion is kept independent from the betatron motion. But the betatron motion is influenced by the synchrotron motion by the momentum dependence of the focussing, which leads to sidebands or satellites of the betatron frequency. Good chromatic corrections are expected to suppress the satellite resonances caused by momentum dependent focussing, and we expect differences for the 6-sextupole family solution and the 2-sextupole family solution.

The parameters of the synchrotron motion are chosen as follows: $U_{rev} = 200$ MV, synchronous phase = 45° which gives in linear approximation together with HERA lattice and optics parameters $h = 10600$, $\alpha = 6.6 \cdot 10^{-4}$ a synchrotron tune of 0.09 for a beam energy of 30 GeV. Thus, with an horizontal tune of $Q_x = 47.16$, we are operating not too far away from the first satellite resonance $Q_x - Q_s = 47$. Results are shown in fig. 4.10 to 4.12 for the quasi-threefold symmetric 2-family and 6-family solutions and the non-symmetric 6-family solution respectively. The plots show the acceptance A_x and $A_x + A_z$ as a function of the synchrotron oscillation amplitude $\Delta\hat{p}/p$.

Comparing the results with those for the static momentum deviation, we see that the global behaviour of the acceptance is compatible with the idea of an average over the static curve in the appropriate momentum range.

It is hard to identify the structure in the curve as the influence of satellite resonances. Because of the non-linearity of the synchrotron restoring force, the synchrotron frequency is expected to decrease with amplitude so that the effect could be identified as the second satellite $Q_x - 2Q_s = 47$. From figs. 4.10 and 4.11 one can't deduce a different strength of satellite resonances for the 2-family and the 6-family solution.

Figure Captions

Fig. 4.1 Non-linear acceptance for the quasi-threefold symmetric optics (a) with a 2-family sextupole distribution versus horizontal tune Q_x (vertical tune Q_z = 47.28 kept constant).

Fig. 4.2 Same as fig. 4.1, 6-family sextupole distribution.

Fig. 4.3 Same as fig. 4.1, non-symmetric optics (b) with 6-sextupole families.

Fig. 4.4 Phase space plot showing 4th integer resonance $4Q_x = 189$.

Fig. 4.5 Phase space plot showing the stabilized 3rd integer resonance $3Q_x = 142$ for the threefold symmetric optics.

Fig. 4.6 Non-linear acceptance for optics (a) with 6-sextupole families versus vertical tune (horizontal tune Q_x = 47.16 kept constant).

Fig. 4.7 Non-linear acceptance versus energy deviation for optics (a) with 2-sextupole families.

Fig. 4.8 Same as fig. 4.7, 6-sextupole families.

Fig. 4.9 Same as fig. 4.7, optics (b) with 6-sextupole families.

Fig. 4.10 Non-linear acceptance versus amplitude of synchrotron oscillations for optics (a) with 2-sextupole families.

Fig. 4.11 Same as fig. 4.10, 6-sextupole families.

Fig. 4.12 Same as fig. 4.10, optics (b) with 6-sextupole families.

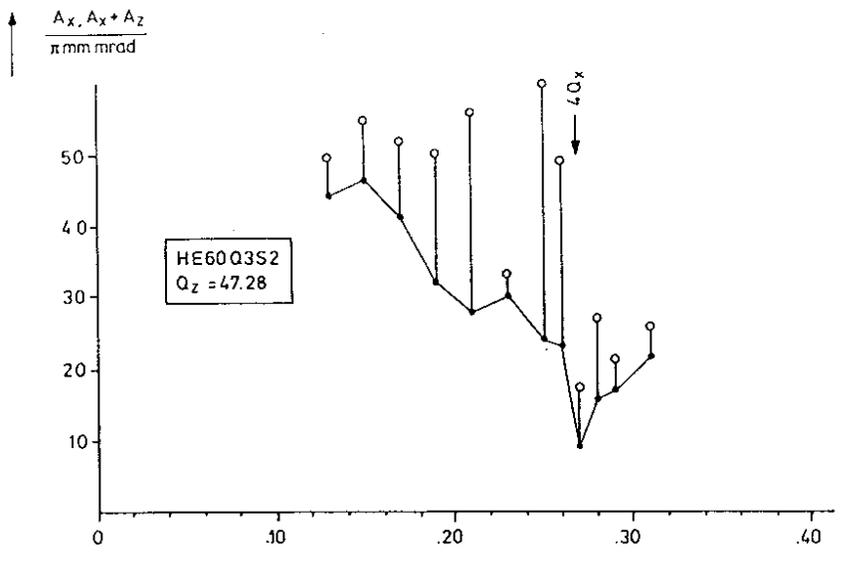

Fig. 4.1

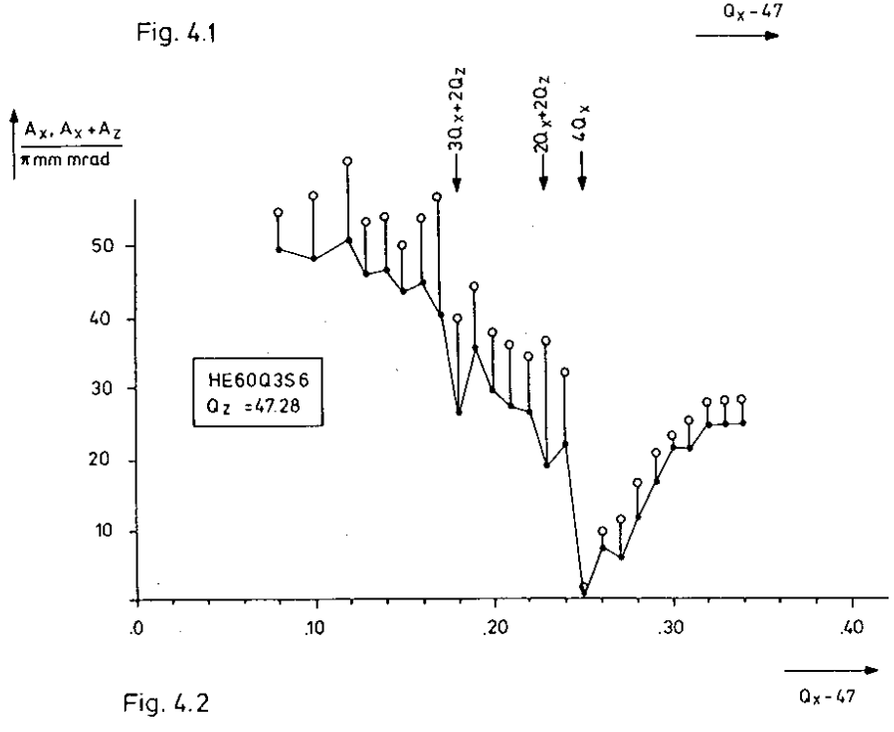

Fig. 4.2

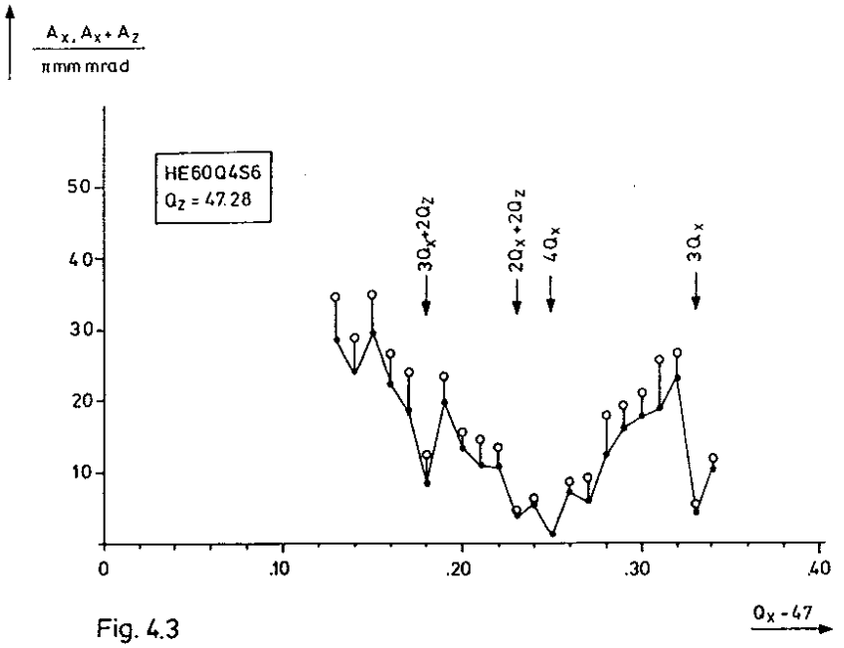

Fig. 4.3

HE600356.ON ENERG.10%COUP.
4TH INTEGER RESONANCE IS DANGEROUS!

Q_x = 47.251

Q_z = 47.280

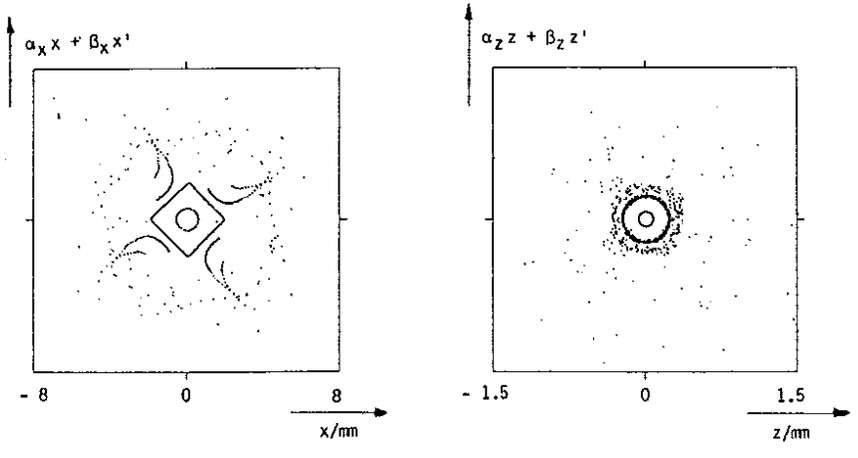

Fig. 4.4

HE600356 NEAR 1/3 INTEGER RESONANCE
STABILIZED BECAUSE IT IS NO STRUCTURE
RESONANCE FOR QUASI 3 FOLD SYMMETRY

Q_x = 47.338

Q_z = 47.280

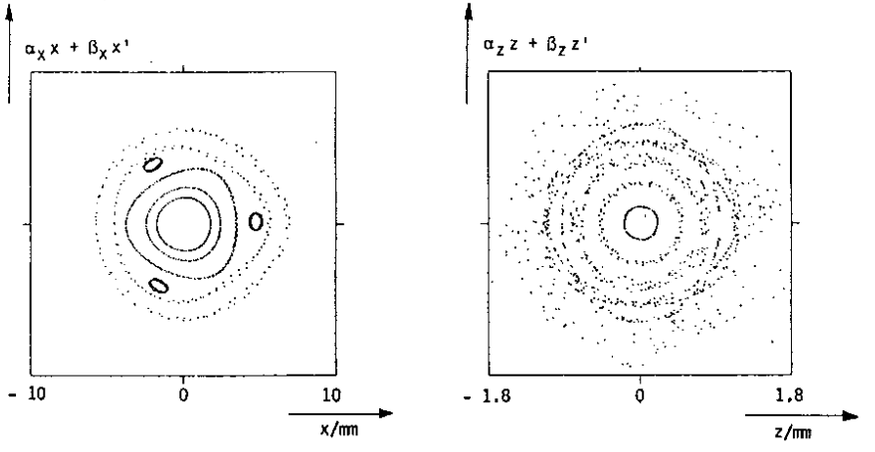

Fig. 4.5

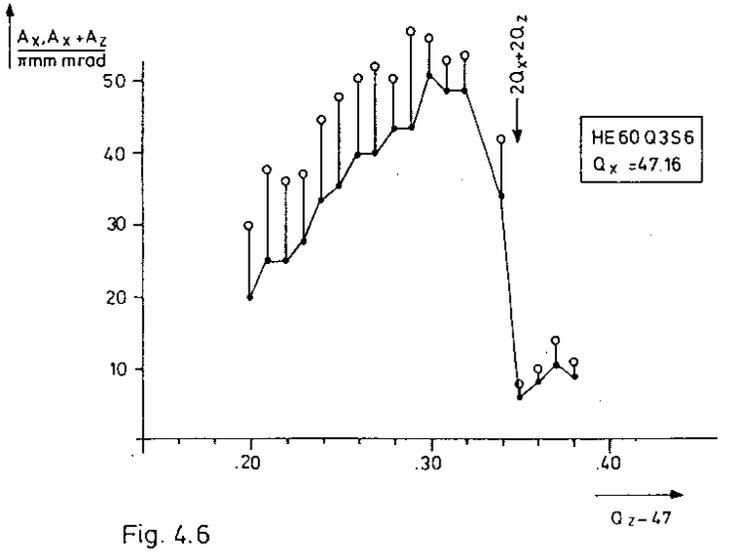

Fig. 4.6

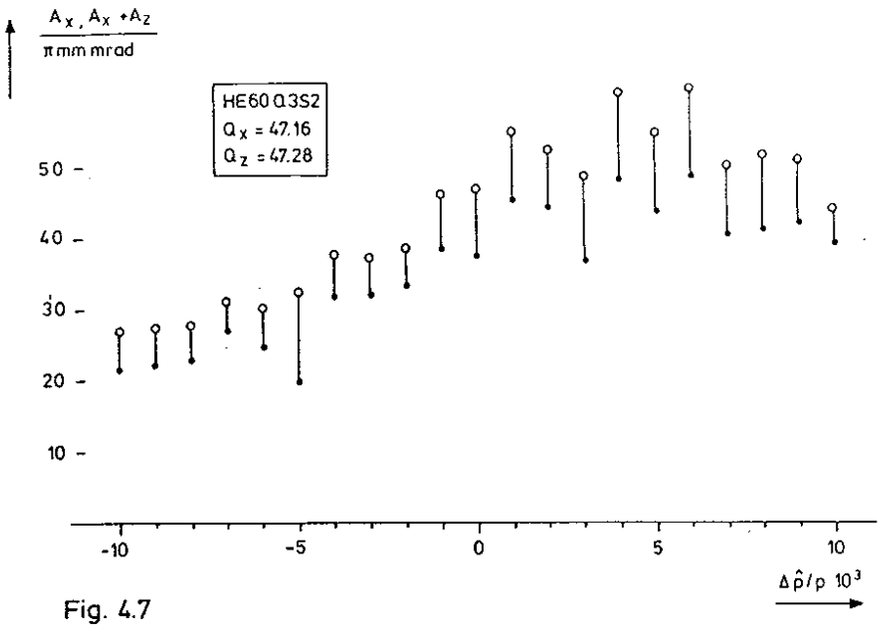

Fig. 4.7

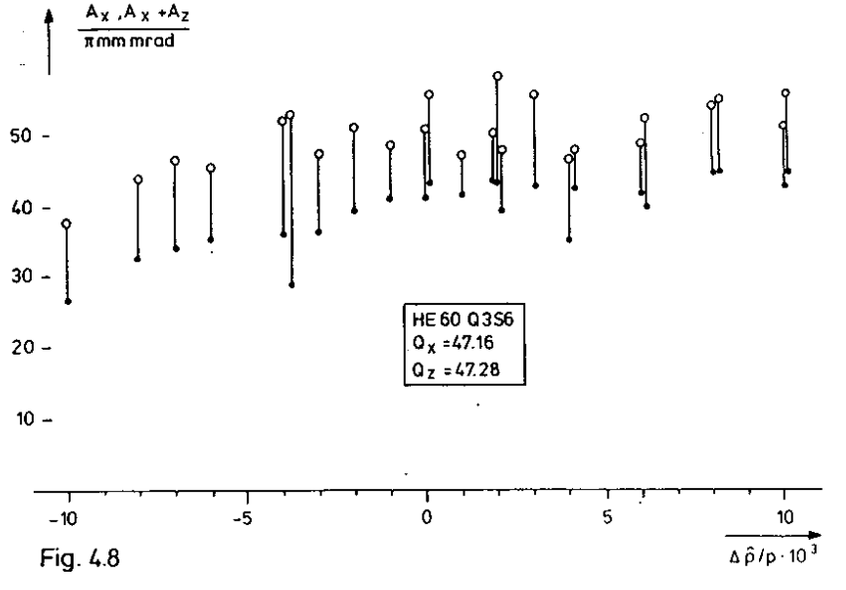

Fig. 4.8

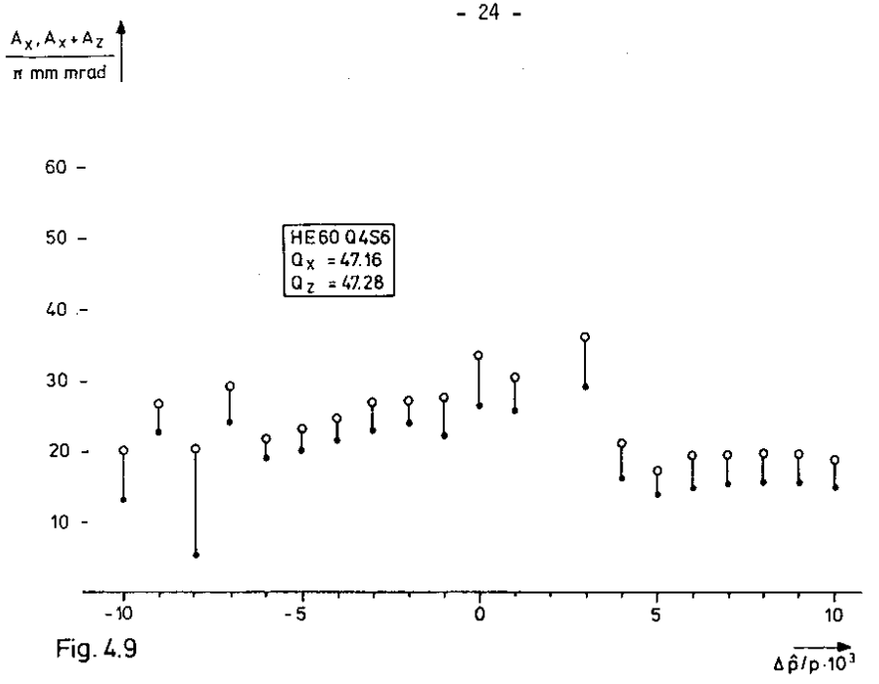

Fig. 4.9

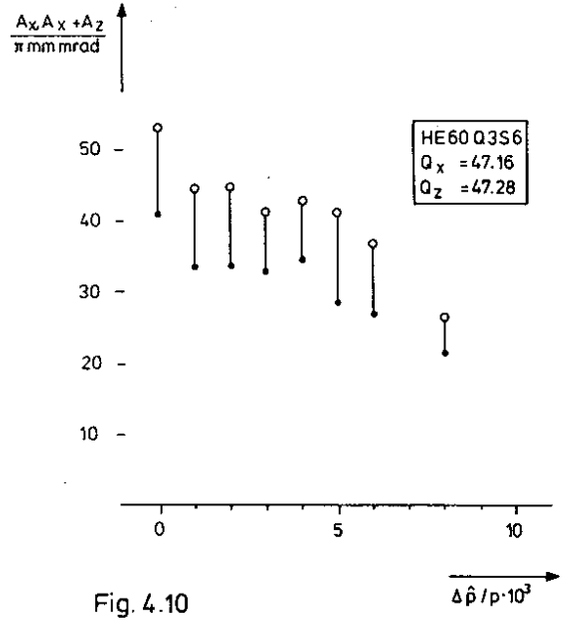

Fig. 4.10

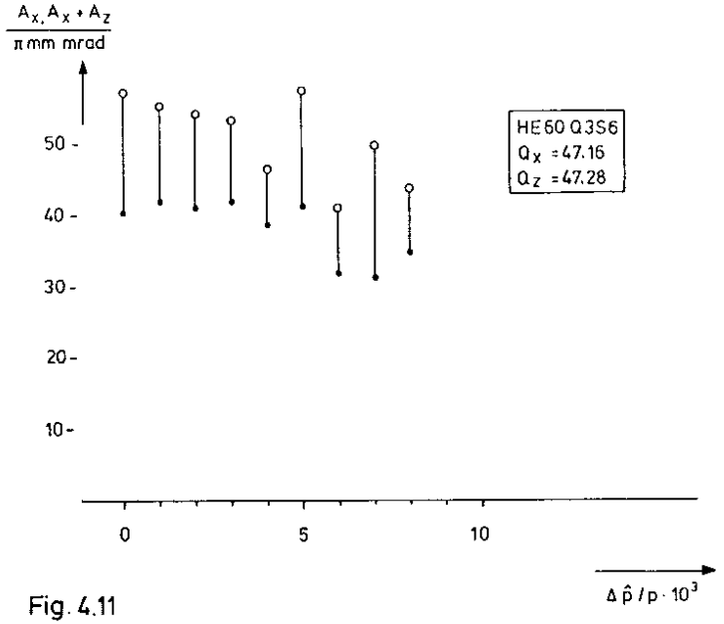

Fig. 4.11

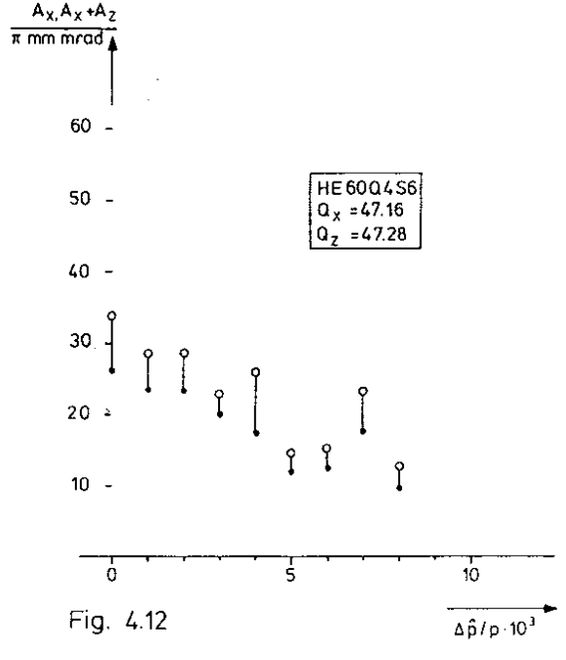

Fig. 4.12

5. Comparison with analytical models

In order to provide an understanding of how the tracking results come about, we compare them with the results of perturbation theory. This comparison is restricted to the case of purely transverse motion. We use the perturbation method as described in reference 4). Here, the Courant-Snyder emittances ε_x and ε_z are expressed as functions of the effective invariants J_x and J_z which have been introduced in section 3, and the Courant-Snyder phase angles. These functions are expanded until quadratic terms in the sextupole strengths. The method provides furthermore the amplitude-dependent tune and the width of resonances excited by linear ("first order") and quadratic terms ("2nd order") in the sextupole strengths.

We start with the comparison of the detuning detained from tracking and obtained from theory. For theoretical calculations the computer code CANOL[6] is used. This comparison is a good check of the range of amplitude in which the non-linear phenomena are described by perturbation theory up to second order.

In first order, the detuning is determined by the integral around the ring of vertical magnetic field components antisymmetric in the horizontal and vertical coordinates (e.g. octupole fields). Because the sextupole fields are even functions of x, there is no first order detuning from sextupoles.

However, in second-order perturbation theory one can assign to each sextupole a virtual non-linear element which describes the interference of that sextupole with all other sextupoles in the ring. This virtual second order element provides the lowest order detuning effect of sextupole fields. It has the form

$$Q_x = Q_{xx} \cdot J_x + Q_{xz} \cdot J_z$$
$$Q_z = Q_{zz} \cdot J_z + Q_{xz} \cdot J_x$$

Results of the comparison are presented in figs. 5.1, 5.2 and 5.3. Plotted is the variation of the tunes with the invariants J_x and J_z in the range between 0 and 20 π mm mrad for $\Delta Q_{x,z}$ vs. $J_{x,z}$ and in the range between 0 and 15 π mm mrad for the cross terms $\Delta Q_{x,z}$ vs. $J_{z,x}$. We recognize that the detuning is qualitatively and quantitatively not very different for the three cases investigated. The horizontal detuning $\Delta Q_x/\Delta J_x$ is described almost perfectly by perturbation theory.

The vertical detuning obtained from tracking shows strong deviations from the linear behaviour while the 4th integer resonance is approached and crossed and the tune locks on to the resonance. Nevertheless, the global behaviour of the vertical detuning is described fairly well by the linear approximation. The vertical detuning is a factor 5 to 10 higher than the horizontal one which is a common property of sextupole systems. The same observations are made with the cross terms $\Delta Q_x/\Delta J_z$, $\Delta Q_z/\Delta J_x$.

So we may conclude that in the emittance range of 0 to 20 mm mrad perturbation theory up to 2nd order is expected to describe the dynamics fairly well provided that the vicinity of resonances is excluded. The latter cases have to be treated properly, selecting single resonance driving terms for the description of the dynamics.

If we compare the resonance driving terms provided by first and second order perturbation theory for the three optical solutions we obtain a better hint to explain the different dynamic apertures found by tracking. In table 5.1, the resonance widths for all 1st and 2nd order sextupole resonances evaluated on the resonance and according to a horizontal emittance of ϵ_x = 10 mm mrad, ϵ_z/ϵ_x = 10 % are shown.

The widths for the non-symmetric solution are for almost every resonance significantly larger than for the quasi-symmetric solutions and this is exactly what one would expect:

If the optics in the arcs were perfectly periodic, no first order sextupole perturbations would be present and second order terms are expected to be small for the 60 deg. lattice. Thus, a major contribution to the resonance driving terms results from the perturbed ß-functions in the matching sections at the ends of the arcs. In the West quadrant, where the matching is very smooth, the contribution to the driving terms is small.

Thus, we have a unity transfer matrix in the West quadrant, not only with respect to the linear off- and on-momentum optics but also with respect to first order non-linear effects. Therefore, we may consider the 3 quadrants remaining as a quasi-threefold symmetric structure for which only the 4th integer resonances $4Q_x$, $4Q_z$ are structure resonances. All other resonances should have considerably smaller strengths than in the non-symmetric cases. The validity of this hypothesis is supported by the analytical calculation of driving terms and, last but not least, by the tracking results.

If one scales the widths of the strongest resonance $Q_x - 2Q_z$ until the dynamic aperture obtained for each of the 3 solutions is reached, one finds in all cases a width of 0.10. Thus, the occurence of the dynamic aperture coincides in all cases with this resonance width, which supports the idea of a maximum tolerable value of this resonance which determines the dynamic aperture.

Furthermore, we should mention that if we scale all the other resonance widths to the dynamic aperture respectively, one finds that for the quasi-symmetric solutions the 2nd order resonances have the same magnitude as the first order ones, whereas the non-symmetric solution is still dominated by first order resonances.

Table 5.1 Resonance widths for ϵ_x = 10 mm mrad, ϵ_z/ϵ_x= 10 %

optics resonances	HE60 Q3S6	HE60 Q3S2	HE60 Q4S6
Q_x = 47	0.0092	0.0089	0.0528
$3Q_x$ = 142	0.0031	0.0085	0.0026
$Q_x + 2Q_z$ = 142	0.0143	0.0099	0.0282
$Q_x - 2Q_z$ = - 47	0.0500	0.0449	0.0631
$2Q_x + 2Q_z$ = 189	0.0030	0.0005	0.0010
$4Q_x$ = 189	0.0026	0.0014	0.0050
$4Q_z$ = 189	0.0003	0.0008	0.0010
$2Q_x$ = 95	0.0007	0.0005	0.0046
$2Q_z$ = 95	0.0066	0.0067	0.0134

We note in addition that the second order resonances have about the same strengths for the threefold symmetric optics with 2- and 6-sextupole families. This means that the perturbed lattice functions at the end of the arcs present a stronger second order distortion than the difference of sextupole strengths for the 6-family distribution.

Figure Captions

Fig. 5.1 Non-linear detuning resulting from tracking (circles) compared to perturbation theory (solid lines) for the threefold symmetric optics (a) with 2-sextupole families.

Fig. 5.2 Same as fig. 5.1, 6-sextupole families.

Fig. 5.3 Same as fig. 5.1, optics (b) with 6-sextupole families.

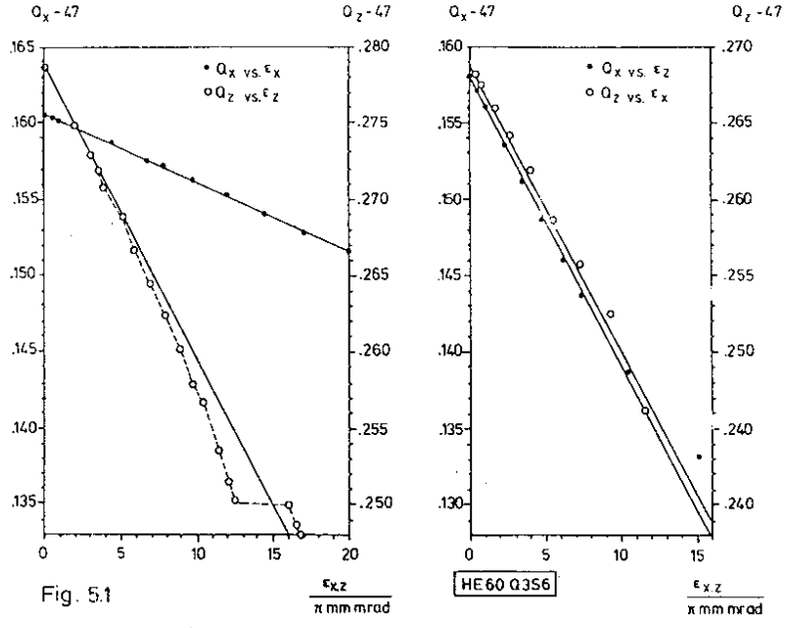

Fig. 5.1

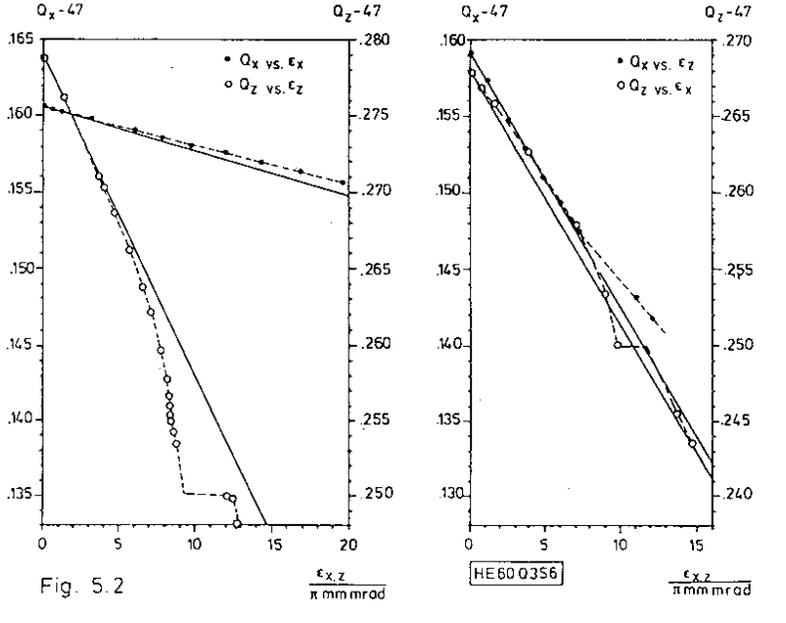

Fig. 5.2

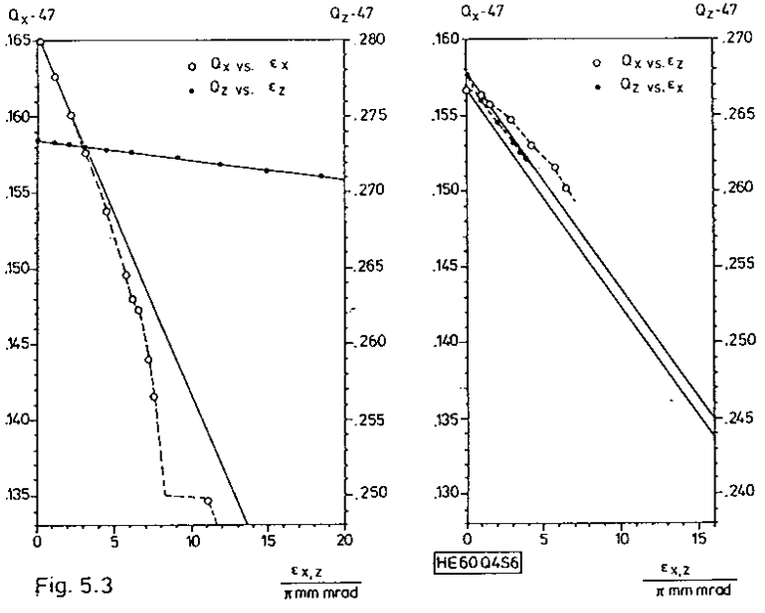

Fig. 5.3

6. Tolerances

It is an interesting question how sensitive the excellent non-linear acceptance of our preferred optical solution is to imperfections in the real machine. We have studied the influence of orbit and gradient errors. For our case, where sextupoles are the only non-linearities, the effects of both sources of errors are similar, namely a distortion of the linear optics. However, orbit deviations in sextupoles differ from random gradient errors in two aspects. First, vertical orbit errors lead to skew quadrupole components which give rise to linear coupling and secondly, orbit deviations at different positions in the lattice are generally correlated[7]. The influence of correlations was investigated by the authors and it was found that for a sextupole distribution with first order cancellation of non-linear distortions (180 degree phase advance between sextupoles of equal strength) it is of minor importance.

For the simulation of orbit errors with the RACETRACK code, a large number of random dipole kicks is generated and adjusted to yield the desired rms orbit deviations $\Delta x,z_{rms}$. Influence of horizontal and vertical distortions were studied individually (fig. 6.1) and in common (see fig. 6.2). The stronger influence of vertical orbit errors can be explained by the fact that these are larger at the positions of the stronger sextupoles. It can be inferred from fig. 6.2 that for a real machine with $\Delta x,z_{rms} < 2$ mm the effect of acceptance reduction does not exceed 20 %.

The influence of random gradient errors was investigated by randomly varying the focussing strengths of the quadrupoles in the arcs. The results (fig. 6.3) show that gradient errors of the order of $\Delta K/K_0 \approx 10^{-3}$ do not lead to a significant acceptance reduction. This could already be expected from the fact that such a gradient error corresponds to an orbit deviation of only about 0.3 mm in a sextupole.

Figure Captions

Fig. 6.1 Non-linear acceptance vs. horizontal (circles) and vertical (squares) rms-orbit distortions for the threefold symmetric optics with 6 sextupole families.

Fig. 6.2 Non-linear acceptance vs. rms-orbit distortions (equal in both planes) for the threefold symmetric optics with 6-sextupole families (two different statistics).

Fig. 6.3 Non-linear acceptance vs. rms-gradient errors for the threefold symmetric optics with 6-sextupole families.

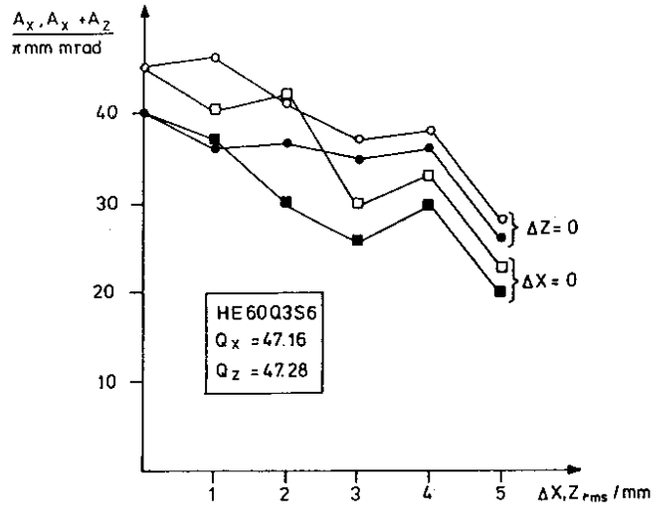

Fig. 6.1

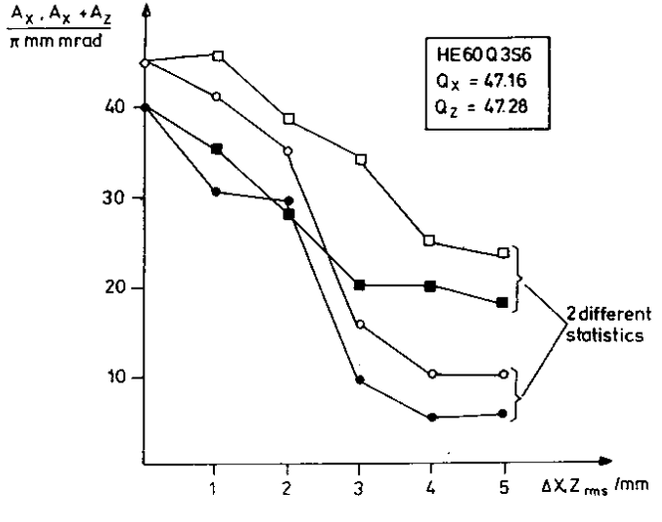

Fig. 6.2

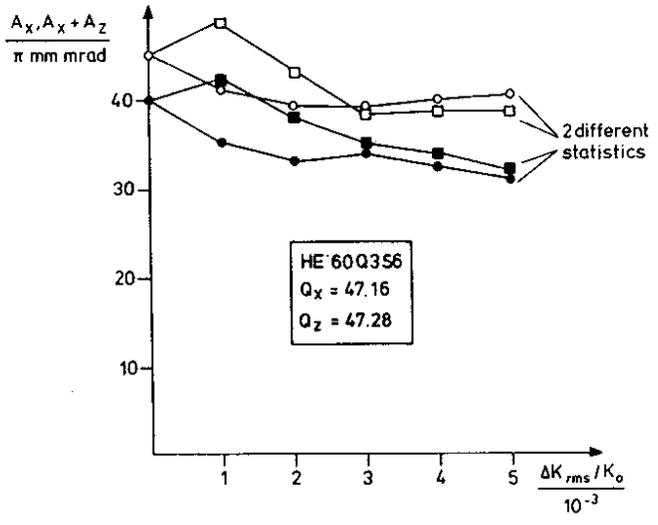

Fig. 6.3

7. Conclusion

The discussion in the previous sections allows the following conclusions:

For the two different linear optics considered, the non-symmetric and the quasi-symmetric solutions, the compensation of chromaticity and the off-energy half-integer stopband is easily accomplished with 6-sextupole families (three for each oscillation plane) resulting in a moderate difference (and therefore in moderate peak values) of the sextupole strengths. ß- and -beat factors at the interaction point vary very little in a momentum range of $\Delta p/p = \pm 1$ %.

With respect to the dynamic aperture, however, the quasi-threefold-symmetric solution is significantly more advantageous. This is the result of numerical simulation of particle motion (tracking). It is explained by the fact that the quasi-threefold symmetry (which is achieved by integer phase advances through the West quadrant, a section which consists of very smooth optics matching sections at the ends of the arc) supresses the lowest order sextupole driven non-linear resonances (which would be excited in the ends of the arcs in north south and east quarters, otherwise). This also avoids the higher order sextupole effects from becoming too strong. These explanations are supported qualitatively and quantitatively by theoretical models.

As a consequence, the dynamic aperture in the threefold-symmetric solution accomodates more than 19 standard deviations of a Gaussian distributed electron beam even for a beam energy of 50 GeV. This provides a large safety factor for the ratio of needed and available aperture.

The solution with 2-sextupole families, which has no half-integer stopband compensation does not give better results for the on-momentum optics. It is explained by the fact that the non-linear effects are produced mainly at the unperiodic ends of the arc, so that the different excitation of the 6-sextupole families is of minor impact.

For particle motion including momentum oscillations the achromatic solution is slightly more stable especially for large momentum amplitude.

We conclude this report with a strong recommendation of the quasi-threefold solution with 6-sextupole families. It should be considered as the standard optical solution and should be the base of all future investigations and design efforts in the HERA e^--ring.

Acknowledgement

The authors wish to thank R. Cooper for carefully reading the manuscript.

References

1) D. Barber, R. Brinkmann, R. Kose, J. Roßbach, K. Steffen and F. Willeke: "HERA Straight Sections for Head-On Electron-Proton Interactions", IEEE Trans. Nucl. Sc. Vol. NS32-5, 1985.

2) A. Wrulich: "Various Sextupole Schemes for the HERA Electron Ring", DESY HERA 85-14, 1985.

3) A. Wrulich: "RACETRACK: A Computer Code for the Simulation of Nonlinear Particle Motion in Accelerators", DESY 84-026, 1984.

4) F. Willeke: "Analytic Study of the TEVATRON Nonlinear Dynamics", Fermilab Report FN422, 1985.

5) F. Schmidt, DESY private communication, 1986.

6) F. Willeke: "CANOL User Guide", to be published.